

Reactions of Laser-Ablated Aluminum Atoms with Nitrogen Atoms and Molecules. Infrared Spectra and Density Functional Calculations for the AlN_2 , Al_2N , Al_2N_2 , AlN_3 , and Al_3N Molecules

Lester Andrews,* Mingfei Zhou,† George V. Chertihin, and William D. Bare

Chemistry Department, University of Virginia, Charlottesville, Virginia 22901

Yacine Hannachi

Laboratoire de Physico-Chimie Moleculaire (CNRS UMR 3805), Universite Bordeaux I, 351, Cours de la Liberation, F-33405 Talence Cedex, France

Received: October 1, 1999

Laser-ablated aluminum atoms react with dinitrogen on condensation at 10 K to form N_3 radical and the subject molecules, which are identified by nitrogen isotopic substitution, further reactions on annealing, and comparison with isotopic frequencies computed by density functional theory. The major AlN_3 product is identified from three fundamentals and a statistically mixed nitrogen isotopic octet pattern. The aluminum rich Al_2N and Al_3N species are major products on annealing to allow diffusion and further reaction of trapped species. This work provides the first experimental evidence for molecular Al_xN_y species that may be involved in ceramic film growth.

Introduction

The importance of aluminum nitride as a semiconductor and ceramic material¹ has led to numerous investigations of the solid material² and its formation by chemical vapor deposition (CVD) from reactions of aluminum alkyls.^{3,4} The only molecular form yet investigated, AlN , has been observed by emission⁵ and investigated by post-Hartree–Fock ab initio calculations.^{6,7} To prepare Al_xN_y species of relevance to the CVD process, laser-ablated Al atoms have been reacted with ammonia.⁸ Such compounds have been modeled by electronic structure calculations.⁹

A recent investigation of laser-ablated Ga atoms and nitrogen revealed a series of Ga_xN_y species that increase stepwise on annealing to allow diffusion and reaction to form Ga_3N and GaN_3 in a manner that might approximate gallium nitride film growth.¹⁰ The stability of similar Al_3N and AlN_3 molecules has been verified by recent electronic structure calculations.¹¹ However, investigations of the B/ N_2 reaction revealed NBNN as the most abundant product.^{12,13} Here follows a combined matrix infrared spectroscopic and density functional theoretical study of novel Al_xN_y molecular species.

Experimental and Computational Methods

The technique for laser ablation and infrared matrix investigation has been described previously.^{12,14,15} The aluminum target (Aesar, 99.998%) was mounted on a rotating rod. The 1064 nm Nd:YAG laser beam (Spectra Physics, DCR-11) was focused on the metal target. Laser energies ranging from 20 to 60 mJ/pulse were used in the experiments. Ablated aluminum atoms were co-deposited with pure nitrogen or 2–4% N_2 mixtures in argon onto a 10 K CsI window at a rate of 2–4 mmol/h for 30

min to 2 h. Nitrogen (Matheson) and isotopic $^{15}\text{N}_2$ (Isotec), $^{14}\text{N}_2$ + $^{15}\text{N}_2$, and $^{14}\text{N}_2$ + $^{14}\text{N}^{15}\text{N}$ + $^{15}\text{N}_2$ (Isotec) mixtures were employed. Infrared spectra were recorded with 0.5 cm^{-1} resolution and 0.1 cm^{-1} accuracy on a Nicolet 750 instrument. Matrix samples were annealed to different temperatures, and selected samples were subjected to broad-band photolysis by a medium-pressure mercury arc lamp (Philips, 175 W) with the globe removed (240–580 nm).

Density functional theory (DFT) calculations were done for potential product molecules expected here using the Gaussian 94 program.¹⁶ Most calculations employed the hybrid B3LYP functional but comparisons were done with the BP86 functional as well.^{17,18} The 6-311+G* basis set was used for both Al and N atoms,¹⁹ and the cc-pVDZ set was employed in several investigations.²⁰ Geometries were fully optimized and frequencies were calculated from analytic second derivatives.

Results

Infrared spectra and density functional calculations of aluminum–nitrogen reaction products will be presented in turn.

Infrared Spectra. Representative infrared spectra are illustrated in Figures 1 and 2 for Al in pure nitrogen for three regions, and product bands are listed in Table 1. The strong N_3 radical^{12,21} absorption at 1657.7 cm^{-1} (not shown) is 13 times stronger than the N_3^- band at 2003.3 cm^{-1} . As a measure of limited oxide contamination, the NO band at 1874.7 cm^{-1} is very weak (A = absorbance = 0.001, not shown) and trace Al_2O is detected at 988.7 cm^{-1} (A = 0.005).²² The major aluminum product absorbs at 2150.9/2144.0 cm^{-1} , 1391.9/1386.0 cm^{-1} , and 509.7 cm^{-1} (not shown) with A = 0.036, 0.006, and 0.004, respectively. Another product has bands at 1501.6 and 956.7 cm^{-1} and another at 777.9/770.3 cm^{-1} , and different products absorb at 656.9 and 650.7 cm^{-1} . Several experiments were done to minimize the NO and Al_2O contamination. Finally, an

* E-mail: lsa@virginia.edu.

† Permanent address: Laser Chemistry Institute, Fudan University, Shanghai, P. R. China.

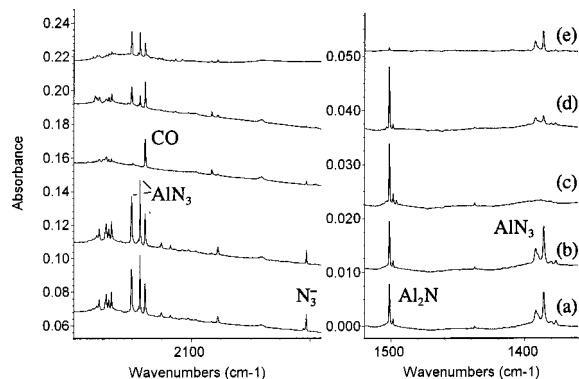


Figure 1. Infrared spectra in the 2200–1900 and 1520–1360 cm⁻¹ regions for laser-ablated Al atoms co-deposited with N₂ at 10 K: (a) sample co-deposited for 30 min; (b) after annealing to 25 K; (c) after 240–580 nm photolysis; (d) after annealing to 30 K; (e) after annealing to 35 K.

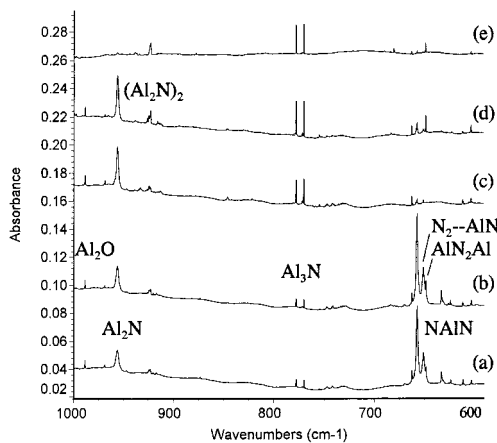


Figure 2. Infrared spectra in the 1000–590 cm⁻¹ region for the same experiment as Figure 1.

experiment with the lowest laser energy used here markedly reduced the 956.7 and 779.9/770.3 cm⁻¹ bands relative to other products.

Similar experiments were done with ¹⁵N₂, and the shifted bands are reported in Table 1. Analogous investigations with ¹⁴N₂ + ¹⁵N₂ and ¹⁴N₂ + ¹⁴N¹⁵N + ¹⁵N₂ mixed isotopic samples gave important diagnostic multiplets. Isotopic spectra are compared in Figures 3–5, and the multiplet absorptions are listed in Table 1.

Experiments were also conducted with 2 and 4% N₂ diluted in argon, and product bands were weaker; Al₂O was detected²² at 992.8 cm⁻¹, but no evidence was found for the major product near 2150 cm⁻¹ in pure nitrogen. Four absorptions in argon are noteworthy: a weak sharp 1991.9 cm⁻¹ band, a broad 1636.1 cm⁻¹ absorption, and features at 924.5 and 773.1 cm⁻¹. The 1991.9 cm⁻¹ band decreased on annealing while the 1636.1 cm⁻¹ band increased and then decreased, and the latter two bands increased and remained through the final annealing. These bands shifted to 1926.3, 1582.4, 900.7, and 753.9 cm⁻¹ with ¹⁵N₂ in argon. An experiment with 2% ¹⁴N₂ + 2% ¹⁵N₂ gave a sharp quartet at 1991.9, 1981.5, 1937.7, 1926.3 cm⁻¹, a 2:1:2 triplet at 924.5, 910.5, 900.7 cm⁻¹, and a doublet at 733.0, 753.9 cm⁻¹. A statistical mixed isotopic sample gave a sharp sextet with additional 1970.5, 1948.4 cm⁻¹ bands, a 1:2:1 triplet at 924.5, 910.5, 900.7 cm⁻¹, and a similar 773.0, 753.9 cm⁻¹ doublet. Several weaker bands are also listed in Table 2. The sharp 1991.9 cm⁻¹ band appears to be due to N₃⁻ and the broader 1636.1 cm⁻¹ absorption to N₃ in solid argon.^{12,21}

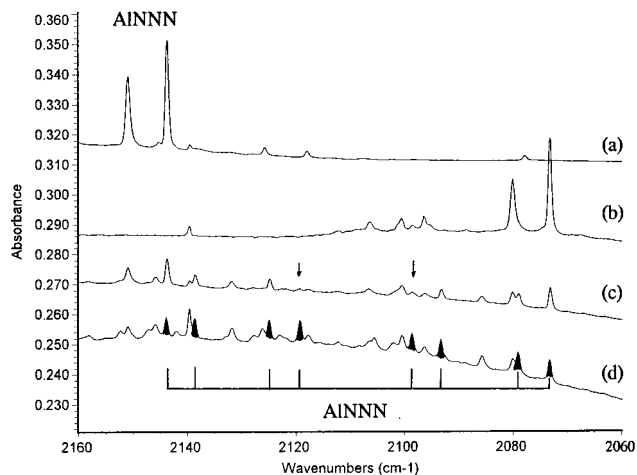


Figure 3. Infrared spectra in the 2160–2060 cm⁻¹ region for pure nitrogen isotopic samples co-deposited with laser-ablated Al atoms after annealing to 25 K: (a) ¹⁴N₂; (b) ¹⁵N₂; (c) 50% ¹⁴N₂ + 50% ¹⁵N₂; (d) 25% ¹⁴N₂ + 50% ¹⁴N¹⁵N + 25% ¹⁵N₂ (major site octet indicated).

TABLE 1: Infrared Absorptions (cm⁻¹) for Laser-Abated Al Atom Reactions with Pure N₂ during Condensation at 10 K

¹⁴ N ₂	¹⁵ N ₂	¹⁴ N ₂ + ¹⁴ N ¹⁵ N + ¹⁵ N ₂	¹⁴ N ₂ / ¹⁵ N ₂	ident
2327.6	2250.3	2327.6, 2289.6, 2250.3	1.03435	N ₂
2178.4	2106.5		1.03413	(N ₂ - -AlN ₃)
2172.3	2100.6		1.03413	(N ₂ - -AlN ₃)
2167.9	2096.4	weak intermediate bands	1.03411	(N ₂ - -AlN ₃)
2150.9	2080.1		1.03404	AlN ₃ site
2144.0	2073.2	2144.0, 2138.7 2125.1, 2119.4, 2098.8, 2093.4, 2079.5, 2073.4	1.03415	AlN ₃
2077.8	2009.6		1.03394	X-N ₃ ⁻
2003.3	1837.5	2003.2, 1992.7, 1981.7, 1959.4, 1948.7, 1937.4	1.03396	N ₃ ⁻
1874.7	1841.8		1.01786	NO
1657.7	1603.5	1657.7, 1649.3, 1640.0, 1621.5, 1613.0, 1603.5	1.03380	N ₃
1501.6	1474.9	1501.6, 1474.9	1.01810	AlNAl
1391.9	1345.4		1.03456	AlN ₃ site
1386.0	1340.2	weak intermediate bands	1.03417	AlN ₃
1132.8	1106.0		1.02423	Al _x N _y
1126.8	1100.4		1.02399	Al _x N _y
1061.9	1040.7		1.0204	Al _x N _y
1054.3	1033.4		1.0202	Al _x N _y
956.7	931.7	956.7, 931.7	1.02683	AlNAl
923.2	899.4	923.2, 909.2, 899.4	1.02646	(Al ₂ N) ₂
777.9	758.6	777.9, 758.6	1.02544	Al ₃ N
770.3	751.2	770.3, 751.2	1.02540	Al ₃ N
680.0	664.9	680.0, 773.0, 664.9	1.02271	Al _x N _y - -(N ₂) _x
656.9	645.4	656.9, 649.5, 645.4	1.01782	NAlN
650.7	636.5	650.7, 636.5	1.02231	N ₂ - -AlN
648.2	634.0	648.2, 640.8, 634.0	1.02240	Al ₂ N ₂
632.7	612.3	632.7, 618.2, 612.3	1.03332	Al _x N _y
623.6	605.8	624, 610, 606	1.02872	Al _x N _y
602.6	589.4	602.6, 589.4	1.02240	Al _x N _y
509.7	501.5		1.01635	AlN ₃
486.7	472.5	486.7, 472.5	1.03005	Al _x N _y

Calculations. Langhoff et al. performed CASSCF and MRCI calculations on the ³Π ground state of AlN and found 744 cm⁻¹ and 1.816 Å and 746 cm⁻¹ and 1.813 Å harmonic frequencies and bond lengths, respectively.⁷ Our B3LYP/6-311+G* calculation gave 730 cm⁻¹ and 1.805 Å for the AlN ground state, which are in very good agreement and serve to “calibrate” the calculations reported here. The B3LYP/cc-pVDZ calculation gave 717 cm⁻¹ and 1.821 Å.

For Al₂N, we considered three isomers, a triangle, AlAlN and AlNAl, and the ²Σ_u⁺ AlNAl species was the most stable

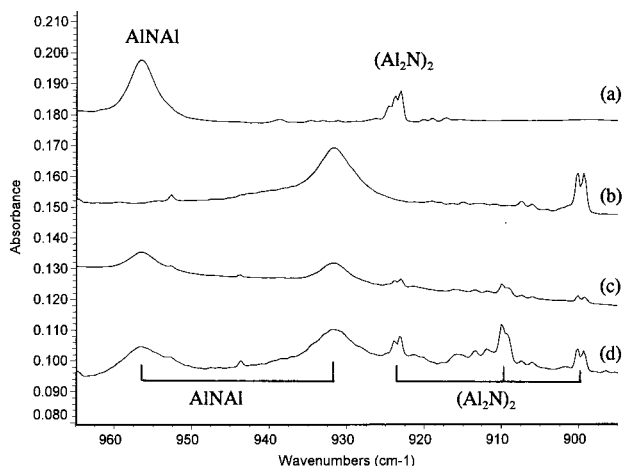


Figure 4. Infrared spectra in the 965–895 cm^{-1} region for same pure nitrogen isotopic samples as in Figure 3.

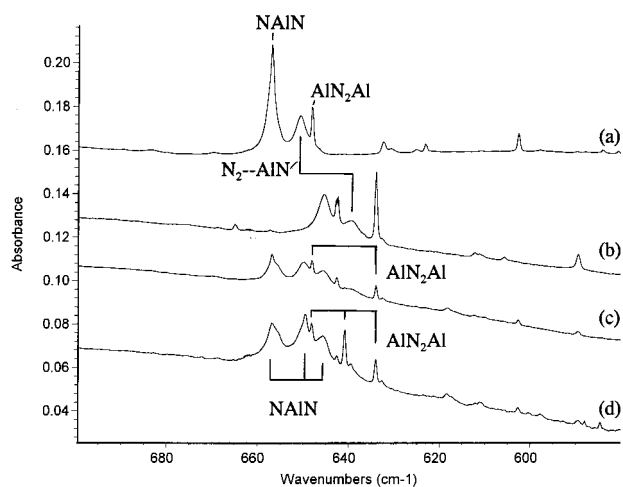


Figure 5. Infrared spectra in the 700–580 cm^{-1} region for same pure nitrogen isotopic samples as in Figure 3.

TABLE 2: Infrared Absorptions (cm^{-1}) for Laser-Abated Al Atom Reactions with N_2 in Excess Argon during Condensation at 10 K^a

¹⁴ N ₂	¹⁵ N ₂	¹⁴ N ₂ + ¹⁴ N ¹⁵ N + ¹⁵ N ₂	¹⁴ N ₂ / ¹⁵ N ₂	anneal, ^b ident
1991.9	1926.3	1991.9, 1981.5, 1970.5, 1948.4, 1937.7, 1926.3	1.03400	–, N ₃ [–]
1636.1	1582.4	covered by water	1.03394	+, N ₃
981.3	955.9	981.3, 955.9	1.02668	–, AlNAl
974.8	949.4	974.8, 949.4	1.02670	–, AlNAl site
924.5	900.7	924.5, 910.5, 900.7	1.02642	+, (Al ₂ N) ₂
773.1	753.9	773.1, 753.9	1.02547	+, Al ₃ N
651.4	637.3	651.4, 644.1, 637.3	1.02212	+, Al ₂ N ₂
601.1	588.1	607.0, 593.7	1.02211	+, Al _x N _y
486.0	472.2	486.0, 479.5, 472.2	1.02922	+, Al _x N _y

^a Similar experiments with 0.3% ¹⁴N₂ and with 0.3% ¹⁵N₂ in neon on a 4 K substrate gave broad 1645.7 and 1590.7 cm^{-1} bands, respectively, for N₃ radical in solid neon. ^b Annealing behavior: – denotes decrease, + denotes increase.

(the C_{2v} form is 54.5 kcal/mol higher and the $C_{\infty v}$ structure 76.6 kcal/mol higher at the B3LYP/cc-pVDZ level). Table 3 shows that the cc-pVDZ set gave slightly longer (0.017 Å) bonds and a 47 cm^{-1} lower antisymmetric stretching frequency than the 6-311+G* set for Al₂N. The Al₂N molecule has a high computed Al–N–Al frequency near that for Al–O–Al.

Following our work with boron where NBNN was the major product species,^{12,13} we calculated NAINN and found (¹A') NAINN to be 73.0 kcal/mol above (¹Σ⁺) AINNN aluminum

azide, presumably owing to weaker Al–N bonds. Our results for AINNN (Table 3) are in accord with recent MP2 calculations.¹¹ Similar B3LYP calculations were done with NBNN and BNNN for comparison, and the boron azide is 34.0 kcal/mol higher. The BNNN stretching frequencies are 2324 cm^{-1} (742 km/mol), 1519 (536), and 979 (128). Also, following our observation of NBN,¹² the aluminum analogue was calculated to have a ⁴Π_u ground state.

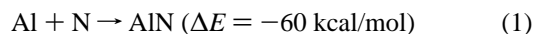
After finding Al₂N to be a stable radical, the saturated Al₃N molecule was computed to be very stable. The Al–N bond lengths and highest frequencies (B3LYP) suggest that the molecule is essentially trigonal planar, in agreement with higher level calculations.¹¹ Figure 6 illustrates the geometries of important Al_xN_y species.

Discussion

The new product absorptions will be identified from isotopic shifts, splitting patterns, and density functional isotopic frequency calculations.

AlN. The first product to be considered is AlN; the gas-phase fundamental is 746.8 cm^{-1} and theoretical calculations sustain this assignment.^{5–7} Although the 670–760 cm^{-1} region contains no significant absorption, a 650.7 cm^{-1} band grows slightly on annealing and almost disappears on photolysis (Figure 2). This band shows a 14/15 isotopic frequency ratio of 1.02231, which is just below the harmonic Al–N diatomic ratio of 1.022 64. Furthermore, the 650.7 cm^{-1} band exhibits a doublet in mixed isotopic spectra providing evidence for a *single* N atom vibration. The gas phase-to-nitrogen-matrix shift is excessive for an isolated molecule so we believe a better assignment for the 650.7 cm^{-1} band is to a perturbed AlN molecule. We note that AlN is a ³Π state and that both NAINN and AlN₃ are singlet states. Although AINNN (see below) increases on annealing, there is no evidence for the higher energy NAINN isomer. Perhaps, the perturbation is at the metal center, i.e., NN–AlN.

The AlN molecule is prepared here by direct reaction 1 between the atoms, which is calculated (B3LYP without ZPE) to be exothermic. The presence of N atoms in these experiments is confirmed by observation of the N₃ radical.^{12,21}



AlN₃. The major aluminum product in solid nitrogen absorbs at 2150.9/2144.0 cm^{-1} , 1391.9/1386.0 cm^{-1} , and 509.7 cm^{-1} . These bands increase 10% on 25 K annealing, almost disappear on 240–580 nm photolysis, reproduce in part on subsequent 30 K annealing, and increase more on 35 K annealing (Figures 1 and 2) The diagnostic mixed isotopic pattern for the strong higher frequency band is a sextet with ¹⁴N₂ + ¹⁵N₂ and an octet with ¹⁴N₂ + ¹⁴N¹⁵N + ¹⁵N₂, which is illustrated in Figure 3 (arrows denote positions of Al-15–14–15 and Al-14–15–14 isotopic bands unique to the statistical mixed isotopic spectrum). These sextet and octet patterns are much clearer for the GaNNN species where annealing increases one matrix site and removes the other;¹⁰ nevertheless, these multiplets identify the vibration of *three inequivalent* nitrogen atoms.

Since this band is in the azide stretching region, AlN₃ was investigated by DFT and found to be a stable ¹Σ⁺ molecule (Table 3). The three strong stretching fundamentals are calculated at 2271.2, 1466.0, and 497.4 cm^{-1} with 6/2/1 relative intensities. Scale factors of 0.947 and 0.949 are required to fit the upper two N–N stretching modes and 1.025 to fit the lower Al–N stretching mode. The same calculation predicted the strong N₃[–] mode at 2078.5 cm^{-1} , which requires a 0.964 scale factor and is appropriate for the B3LYP functional.²³ The

TABLE 3: Calculated (B3LYP/6-311+G*) Geometry, Frequencies (cm⁻¹), and Intensities (km/mol) for the AlN, Al₂N, Al₃N, NAIN, NAINN, AINNN, Al₂N₂, and Al₃N₂ Molecules

molecule	geometry	frequencies (intensities)
AlN (³ Π)	Al–N: 1.805 Å	730.1 (12) 713.9 (12) ^a
Al ₂ N (² Σ _u ⁺)	Al–N: 1.731 Å linear	131.8 (35), 524.9 (0), 1051.4 (97) 128.3 (33), 524.9 (0), 1023.3 (92) ^a
Al ₂ N (² Σ _u ⁺) ^b	Al–N: 1.748 Å linear	77.7 (2 × 15), 509.2 (0), 1004.3 (72) ^b 75.6, 509.2, 977.4 ^a
Al ₂ N ⁻ (¹ Σ _g ⁺)	Al–N: 1.746 Å linear	119.0 (2 × 2), 518.7 (0), 1129.8 (685) 115.8 (1 × 2), 518.7 (0), 1099.5 (643) ^a
Al ₃ N (¹ A ₁) C _{2v}	Al ₁ N: 1.8495 Å Al _{2,3} N: 1.850 Å ∠Al ₂ –N–Al ₃ : 120.1°	153.8 (3), 154.3 (3), 217.0 (0), 427.5 (0), 751.5 (328), 751.9 (329) 153.2 (3), 153.8 (3), 210.8 (0), 427.5 (0), 732.4 (312), 732.8 (314) ^a
Al ₃ N (¹ A ₁) D _{3h} ^c	Al–N: 1.863 Å	141.1 (3 × 2), 200.6 (0.1), 414.3 (0), 731.9 (309 × 2) ^c
NAIN (⁴ Π _u)	Al–N: 1.804 Å linear	122.2 (43), 146.2 (86), 643.2 (0), 725.7 (582) 120.2 (41), 143.8 (83), 621.5 (0), 713.8 (563) ^a
NAINN (¹ A')	N–Al: 1.746 Å Al–N: 2.021 Å N–N: 1.106 Å N–Al–N: 87.1° Al–N–N: 177.7°	89.8 (47), 230.6 (4), 259.0 (17), 326.4 (12), 840.1 (21), 229.6 (381)
AINNN (¹ Σ ⁺)	Al–N: 1.826 Å N–N: 1.206 Å N–N: 1.138 Å	94.4 (2), 497.4 (167), 625.4 (17), 626.4 (18), 1466.0 (320), 2271.2 (1018) 91.6 (2), 490.8 (162), 604.2 (16), 605.2 (17), 1416.9 (301), 2194.4 (950) ^a
N ₃ ⁻ (¹ Σ _g ⁺)	1.1832 Å	628.2 (7 × 2), 1351.8 (0), 2078.5 (1241)
AlN ₂ Al (³ Σ _g ⁻)	Al–N: 1.860 Å N–N: 1.204 Å	82.2 (2), 257.7 (0), 369.2 (0), 634.3 (579), 1739.4 (0)
AlN ₂ Al (³ Σ _g ⁻) ^b	Al–N: 1.888 Å N–N: 1.204 Å	78.4 (1 × 2), 224.9 (0 × 2), 355.9 (0), 612.0 (509), 1757.1 (0) ^b 76.7 (π _u), 217.5 (π _g), 355.9 (π _g), 598.5 (σ _u), 1697.8 (σ _g)
(AlN) ₂ (¹ A _g)	Al–N: 2.041 Å N–N: 1.267 Å	160.4 (0.2), 195.3 (21), 337.0 (0), 554.2 (0), 571.5 (509), 1445.9 (0) 156.9 (0.2), 191.0 (20), 337.0 (0), 536.5 (0), 558.9 (487), 1396.8 (0)
(AlN) ₂ (¹ A _g) ^b	Al–N: 2.074 Å N–N: 1.263 Å	156 (0), 193 (18), 331 (0), 553 (0), 564 (463), 1453 (0) ^b
Al ₃ N ₂ (² Σ _u ⁺)	Al–N: 1.705 Å N–Al: 1.713 Å	30.2 (10 × 2) (π _u), 123.9 (0) (π _g), 223.4 (82 × 2) ((π _u)) 375.9 (0) (σ _g), 664.3 (230), (π _u), 1161.7 (0) (σ _g), 1178.2 (π _u)

^a Frequencies for ¹⁵N substitution. ^b cc-pVDZ basis set. ^c BP86 functional.

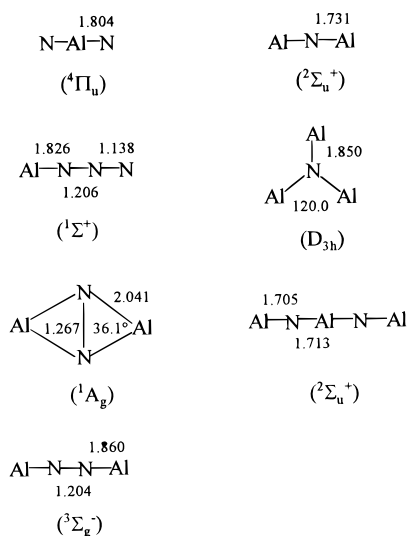
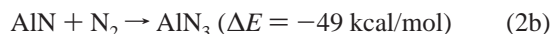
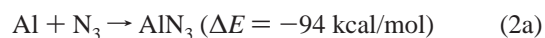


Figure 6. Optimized geometries of Al₃N_y products computed by B3LYP/6-311+G*. Bond lengths are in ångstroms, and angles, in degrees.

relative intensities are also modeled reasonably well by the B3LYP functional except the intensity of the weaker symmetric N–N–N stretching mode is overestimated relative to the stronger antisymmetric N–N–N stretching mode. The calculated and observed 14/15 isotopic ratios match and verify the normal mode assignments. Similar agreement between experiment and theory was found for GaN₃.¹⁰ The gas phase observation of CaN₃ and SrN₃, our matrix formation of the MN₃ (M = Al, Ga, In, Tl) molecules, and the synthesis of Al(N₃)₃ show that these azides are physically stable molecules.^{10,24,25}

Two mechanisms for the formation of AlN₃ come to mind, the reaction of Al with the N₃ radical and the AlN reaction with N₂, the strongly exothermic (B3LYP) reactions 2a and 2b.



Mixed ¹⁴N₂ + ¹⁵N₂ isotopic spectra can in principle distinguish between these two reactions, but complications from two matrix site absorptions reduce the accuracy of band intensity measurements. However, for GaN₃, the mixed isotopic spectra were clearly resolved for the major site absorption, and it was suggested that about 80% of the GaN₃ product is formed from the N₃ radical reaction.¹⁰

NAIN. The strong 656.9 cm⁻¹ band also increased on annealing and decreased markedly on photolysis (Figure 2). This band showed a small ¹⁴N/¹⁵N ratio (1.017 82) and an approximate 1:2:1 triplet pattern with ¹⁴N₂ + ¹⁴N¹⁵N + ¹⁵N₂, which is characteristic of two equivalent N atoms. In fact the 14/15 isotopic ratio for the harmonic antisymmetric vibration of a linear N–Al–N unit is 1.016 73. Our B3LYP calculations find a stable linear NAIN molecule (⁴Π_u state) with the σ_u frequency at 725.7 cm⁻¹, in very good agreement with the matrix observation. The slightly higher observed 14/15 ratio might suggest a slight bending of the molecule in the matrix. The scale factor 0.905 required to fit the calculated and observed bands is lower than other comparisons reported here; this suggests that higher level calculations might provide a better description of the ⁴Π_u state of NAIN.

The NAIN molecule is formed by the reaction of N with the metal center in AlN, reaction 3, which is exothermic. However,

NAlN is higher in energy than Al + N₂ by 120 kcal/mol (B3LYP), but NAlN clearly is kinetically stable. Even Al–N₂ is a van der Waals molecule (bound 4 kcal/mol as estimated by B3LYP).



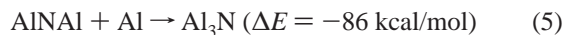
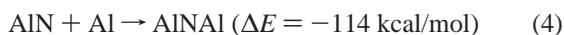
The analogous NGaN molecule was observed at 586.4, 584.1 cm⁻¹ (⁶⁹Ga, ⁷¹Ga) where resolved isotopic splitting confirmed the vibration of a single gallium atom.¹⁰

AlNAI. The 956.7 cm⁻¹ band increases slightly on annealing but almost *doubles* on photolysis. The mixed isotopic spectra reveal a doublet absorption for the vibration of a *single* nitrogen atom and a large (1.02683) nitrogen 14/15 isotopic ratio. In fact the 14/15 isotopic ratio for the harmonic antisymmetric vibration of a linear Al–N–Al unit is 1.027 50. Our B3LYP calculation finds the most stable Al₂N species to be linear AlNAI (²Σ_u⁺) with the calculated σ_u mode at 1051.4 cm⁻¹, in very good agreement with the matrix spectrum. The scale factor 0.910 again suggests that higher level calculations might produce a better fit, and indeed, the cc-pVDZ basis set (Table 3) produces a 1004.3 cm⁻¹ σ_u frequency in better agreement with the observed value (0.953 scale factor). The 956.7 cm⁻¹ band is assigned to AlNAI in solid nitrogen.

The sharp 1501.6 cm⁻¹ band tracks with the 956.7 cm⁻¹ band on annealing and photolysis, and it too shows the doublet mixed isotopic spectrum for the vibration of a *single* nitrogen atom. Its appearance in the NO region and 14/15 isotopic ratio invited consideration of such a species but AlNO and AlON absorb elsewhere.²⁶ The differences 1501.6–956.7 = 544.9 cm⁻¹ and 1474.9–931.7 = 543.2 cm⁻¹ for the ¹⁵N counterpart provide a mode that shows *very little* ¹⁵N-shift and is near the 524.9 cm⁻¹ calculated value for the σ_g mode of AlNAI. A slight amount of bending of the molecule would decrease the 14/15 ratio of the σ_u mode and increase the 14/15 ratio of the σ_g mode. Although the 1501.6 cm⁻¹ band absorbance (0.008) is larger relative to the 956.7 cm⁻¹ band (0.014) than normally found for a combination band and a fundamental, linear molecules often have relatively strong combination bands, and the 1501.6 cm⁻¹ band is assigned to the σ_u + σ_g combination band for AlNAI.

The argon matrix spectra reveal weak 981.3, 974.8 cm⁻¹ bands with the same isotopic behavior that can be assigned to AlNAI in solid argon. This suggests a matrix shift for the pure nitrogen environment, and the argon matrix bands clearly fit the DFT frequency calculations better.

The sequential reactions of Al atoms with AlN are exothermic, based on our B3LYP calculations.



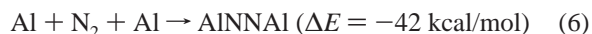
Al₃N. Two sharp bands at 777.9, 770.3 cm⁻¹ also increased slightly on annealing, but markedly on photolysis, more on subsequent annealing, and remained strong after 35 K annealing, in contrast to the case with AlNAI, where they almost disappeared (Figure 2). Only the same pure isotopic bands were observed in mixed isotopic experiments; so again a *single* nitrogen atom is involved. These bands exhibited virtually the same isotopic 14/15 ratio, 1.025 42 ± 0.000 02, which is slightly smaller than the above 956.7/931.7 ratio for AlNAI. Hence, the 777.9, 770.3 cm⁻¹ bands are also due to an antisymmetric Al–N–Al stretching mode, with a slightly smaller included angle, and the product may involve further Al reaction with AlNAI.

Our B3LYP and BP86 and recent higher level calculations¹¹ show that Al₃N is stable, and the strong e' mode predicted at 751.7 cm⁻¹ with 14/15 ratio 1.026 06 is extremely close to the observed value. The 777.9, 770.3 cm⁻¹ bands are assigned to the e' mode of Al₃N split by interaction with the nitrogen matrix.

The major product in argon matrix experiments at 773.1 cm⁻¹ increases and remains on annealing to 40 K. The sharp doublet with mixed isotopic precursor and the 1.025 47 isotopic frequency ratio show that this is the same Al₃N species observed in the nitrogen matrix. Finally, the observation of a single band for the e' mode of Al₃N in solid argon shows that the splitting in the nitrogen matrix is environmental and suggests that the split mode in the B3LYP calculation is due to symmetry breaking inherent in the calculation.²⁷ The D_{3h} symmetry of the molecule maintained with the pure density functional BP86 (Table 3) is also expected in the gas phase.

Al₂N₂. The most stable Al₂N₂ isomer is the (¹A₁') rhombic ring,¹¹ and this characteristic (AlN)₂ structure exhibits diatomic isotopic ratios. However, the linear AlNNAI molecule is only 1.8 kcal/mol higher at the B3LYP level with both basis sets, and the σ_u mode also exhibits the diatomic isotopic ratio. The sharp 648.2 cm⁻¹ band meets these requirements: a 1.022 40 isotopic ratio and a triplet with ¹⁴N₂ + ¹⁴N¹⁵N + ¹⁵N₂ for *two equivalent* nitrogen atoms. The b_{1u} mode of the singlet rhombus is predicted at 571.5 cm⁻¹, whereas the σ_u mode of triplet AlNNAI is 634.3 cm⁻¹ (Table 3). Clearly, the latter fits the 648.2 cm⁻¹ band more closely, and it is assigned accordingly.

Note, however, that a strong 648.2, 634.0 cm⁻¹ doublet is observed with ¹⁴N₂ + ¹⁵N₂, indicating that a *single dinitrogen* molecule is reacting to form AlNNAI. Although Al–N₂ is only a van der Waals molecule, another Al atom will react to give the stable AlNNAI product, reaction 6, which is 42 kcal/mol exothermic.



The 651.4 cm⁻¹ argon matrix band exhibits the same isotopic behavior and is likewise assigned to AlNNAI.

The 680.0 cm⁻¹ nitrogen matrix band increases on late annealing at the expense of the 648.2 cm⁻¹ band (Figure 2). The mixed isotopic triplet and 14/15 ratio are also in accord with an Al₂N₂ assignment, but this species is probably aggregated by additional molecules, possibly more extensively coordinated by N₂.

(Al₂N)₂. Both nitrogen and argon matrix experiments contain a weak band near 924 cm⁻¹ that grows on annealing and remains at the end of annealing cycles. In the nitrogen matrix these bands form 1:2:1 triplets in *both* mixed isotopic experiments so *two equivalent* nitrogen atoms from *different* nitrogen molecules are required. The 14/15 ratios 1.0264 also denote the antisymmetric Al–N–Al vibration of nearly linear Al–N–Al subunits. The annealing behavior suggests a high Al/N species. The 924 cm⁻¹ bands are probably due to an (Al₂N)₂ dimer formed from two Al₂N radicals, reaction 7.



In the argon matrix with ¹⁴N₂ + ¹⁵N₂, the 2:1:2 triplet suggests the participation of another mechanism involving a single N₂ unit and implies that four Al atoms may be able to react with one N₂ molecule, reaction 8.



Higher Al_xN_y Absorptions. The nitrogen matrix experiments contain bands at 1132.8, 1126.8, 1061.9, and 1054.3, which increase on annealing and show 14/15 isotopic ratios near the diatomic AlN value. Unfortunately, no mixed isotopic data can be obtained from this congested spectral region. The 1132.8, 1126.8 cm⁻¹ bands are destroyed by photolysis while the 1061.9, 1054.3 cm⁻¹ bands increase and remain on final annealing. Clearly, these bands are due to higher Al_xN_y clusters. In this regard a linear AlNAlNAl chain has a very strong stretching mode predicted at 1178 cm⁻¹ with a 14/15 ratio 1.0230, which suggests that Al_xN_y chains absorb in this region.

Conclusions

Laser-ablated aluminum atoms react with dinitrogen on condensation at 10 K to form the N₃ radical and the AlN₂, Al₂N, Al₂N₂, AlN₃, and Al₃N molecules, which are identified by nitrogen isotopic substitution, further reactions on annealing, and comparison with isotopic frequencies computed by density functional theory. The major AlN₃ product is identified from three fundamentals and a statistically mixed nitrogen isotopic octet pattern. The aluminum rich Al₂N and Al₃N species are major products on annealing to allow diffusion and further reaction of trapped species. The calculated Al–N bond length is shorter for Al₂N but longer for Al₃N than for AlN. Complementary argon matrix experiments favor the aluminum rich Al₂N, Al₃N, and (Al₂N)₂ species and, accordingly, fail to produce AlN₃, the major product in pure dinitrogen experiments. This work provides the first experimental evidence for molecular Al_xN_y species that may be involved in ceramic film growth.

Acknowledgment. We gratefully acknowledge partial research support from the NSF, PRF, and CNRS.

References and Notes

- (1) Morz, T. J., Jr. *Ceram. Bull.* **1991**, *70*, 849.
- (2) See for example: (a) Pandey, R.; Sutjianto, A.; Seel, M.; Jaffe, J. E. *J. Mater. Res.* **1993**, *8*, 1992. (b) Miwa, K.; Fukumoto, A. *Phys. Rev. B* **1993**, *48*, 789. (c) Ueno, M.; Onodera, A.; Shimomura, O.; Takemura, K. *Phys. Rev. B* **1992**, *45*, 10123. (d) Ruiz, E.; Alvarez, S.; Alemarz, P. *Phys.*

Rev. B Cond. Matter **1994**, *94*, 7115. (e) Knudsen, A. K. *Bull. Am. Ceramic Soc.* **1995**, *74*, 97. (f) Krupitskaya, R. Y.; Auner, G. W. *J. Appl. Phys.* **1998**, *84*, 2861. (g) Kiehne, G. T.; Wong, G. K. L.; Ketterson, J. B. *J. Appl. Phys.* **1998**, *84*, 5922.

- (3) *Chemistry of Aluminum, Gallium, Indium and Thallium*; Downs, A. J., Ed.; Chapman and Hall: New York, 1993.
- (4) Timoshkin, A. Y.; Bettinger, H. F.; Schaefer, H. F., III. *J. Am. Chem. Soc.* **1997**, *119*, 5668.
- (5) Simmons, J. D.; McDonald, J. K. *J. Mol. Spectrosc.* **1972**, *41*, 584.
- (6) Pelissier, M.; Malrieu, J. P. *J. Mol. Spectrosc.* **1979**, *77*, 322.
- (7) Langhoff, S. R.; Bauschlicher, C. W., Jr.; Petterson, L. G. M. *J. Chem. Phys.* **1988**, *89*, 7354.
- (8) Lanzisera, D. V.; Andrews, L. *J. Phys. Chem. A* **1997**, *101*, 5082.
- (9) Davy, R. D.; Jaffrey, K. L. *J. Phys. Chem.* **1994**, *98*, 8930.
- (10) Zhou, M. F.; Andrews, L. *J. Phys. Chem. A*, in press.
- (11) Boo, B. H.; Liu, Z. *J. Phys. Chem. A* **1999**, *103*, 1250.
- (12) Hassanzadeh, P.; Andrews, L. *J. Phys. Chem.* **1992**, *96*, 9177.
- (13) Andrews, L.; Hassanzadeh, P.; Burkholder, T. R.; Martin, J. M. L. *J. Chem. Phys.* **1993**, *98*, 922.
- (14) Burkholder, T. R.; Andrews, L. *J. Chem. Phys.* **1991**, *95*, 8697.
- (15) Andrews, L.; Burkholder, T. R.; Yustein, J. T. *J. Phys. Chem.* **1992**, *96*, 10182.
- (16) Frisch, M. J.; Trucks, G. W.; Schlegel, H. B.; Gill, P. M. W.; Johnson, B. G.; Robb, M. A.; Cheeseman, J. R.; Keith, T.; Petersson, G. A.; Montgomery, J. A.; Raghavachari, K.; Al-Laham, M. A.; Zakrzewski, V. G.; Ortiz, J. V.; Foresman, J. B.; Cioslowski, J.; Stefanov, B. B.; Nanayakkara, A.; Challacombe, M.; Peng, C. Y.; Ayala, P. Y.; Chen, W.; Wong, M. W.; Andres, J. L.; Replogle, E. S.; Gomperts, R.; Martin, R. L.; Fox, D. J.; Binkley, J. S.; Defrees, D. J.; Baker, J.; Stewart, J. P.; Head-Gordon, M.; Gonzalez, C.; Pople, J. A. *Gaussian 94*, Revision B.1; Gaussian, Inc.: Pittsburgh, PA, 1995.
- (17) Lee, C.; Yang, E.; Parr, R. G. *Phys. Rev. B* **1988**, *37*, 785.
- (18) Perdew, J. P. *Phys. Rev. B* **1986**, *33*, 8822.
- (19) Becke, A. D. *J. Chem. Phys.* **1993**, *98*, 5648. Mclean, A. D.; Chandler, G. S. *J. Chem. Phys.* **1980**, *72*, 5639. Krishnan, R.; Binkley, J. S.; Seeger, P.; Pople, J. A. *J. Chem. Phys.* **1980**, *72*, 650.
- (20) Woon, D. E.; Dunning, T. H., Jr. *J. Chem. Phys.* **1993**, *98*, 1358.
- (21) Tian, T.; Facelli, J. C.; Michl, J. *J. Phys. Chem.* **1991**, *95*, 8554.
- (22) Sonchik, S. M.; Andrews, L.; Carlson, K. D. *J. Phys. Chem.* **1983**, *87*, 2004 and references therein.
- (23) Bytheway, I.; Wong, M. W. *Chem. Phys. Lett.* **1998**, *282*, 219.
- (24) Brazier, C. R.; Bernath, P. F. *J. Chem. Phys.* **1988**, *88*, 2112.
- (25) Linnen, C. J.; Macks, D. E.; Coombe, R. D. *J. Phys. Chem. B* **1997**, *101*, 1602.
- (26) Andrews, L.; Zhou, M. F.; Bare, W. D. *J. Phys. Chem.* **1998**, *102*, 5019.
- (27) Sherill, C. D.; Lee, M. S.; Head-Gordon, M. *Chem. Phys. Lett.* **1999**, *302*, 425.